

Behavior of quantum discord, local quantum uncertainty, and local quantum Fisher information in two-spin-1/2 Heisenberg chain with DM and KSEA interactions

Anna V. Fedorova · M. A. Yurischev*

Received:

Abstract A two-qubit Heisenberg XYZ model with Dzyaloshinsky–Moriya (DM) and Kaplan–Shekhtman–Entin-Wohlman–Aharony (KSEA) interactions is considered at thermal equilibrium. Analytical formulas are derived for the local quantum uncertainty (LQU) and local quantum Fisher information (LQFI). Using the available expressions for the entropic quantum discord, we perform a comparative study of these measures of nonclassical correlation. Our analysis showed the following: all three measures of quantum correlation have similar qualitative and even quantitative behavior on temperature for different values of system parameters, there are regions in the parameter space which correspond to a local increase of correlations with increasing temperature, and sudden changes in the behavior of quantum correlations occur at certain values of the interaction parameters.

Keywords · Heisenberg spin model · Density matrix · Quantum correlations · Discord · Local quantum uncertainty · Quantum Fisher information

1 Introduction

The concept of quantum information correlation is central to modern quantum information science. Until the 21st century, quantum correlation meant entanglement. It manifests itself in the Einstein-Podolsky-Rosen gedanken (thought) experiment, Bell’s inequality test, quantum cryptography, superdense coding,

A. V. Fedorova
Institute of Problems of Chemical Physics, Russian Academy of Sciences, Chernogolovka
142432, Moscow Region, Russia
E-mail: panna@icp.ac.ru

M. A. Yurischev
Institute of Problems of Chemical Physics, Russian Academy of Sciences, Chernogolovka
142432, Moscow Region, Russia
E-mail: yur@itp.ac.ru

teleportation, etc. [1,2] (see also review articles [3,4,5,6]). Quantum correlations are considered as a physical resource (“as real as energy” [5])¹. This statement requires a mathematical definition, since, according to Kant, “in jeder besonderen Naturlehre nur so viel eigentliche Wissenschaft angetroffen werden könne, als darin Mathematik anzutreffen ist” (“in any special doctrine of nature there can be only as much *proper* science as there is *mathematics* therein” or “every natural science contains as much truth as much mathematics it contains”). Quantum entanglement was quantified in 1996, first for pure states [8,9], and then for mixed states [10]. According to the accepted definition, the entanglement of a bipartite pure state is the von Neumann entropy either of the two subsystems.² The entanglement (of formation) of a bipartite mixed state is defined as the minimum entanglement of an ensemble over all ensembles realizing the mixed state.

At one time it was believed that quantum entanglement is the main ingredient of quantum speedup in quantum computation and communication, but there was no strong evidence. Moreover, in 1998, Knill and Laflamme showed, using the model of deterministic quantum computation with one pure qubit (DQC1) [12], that computation can achieve an exponential improvement in efficiency over classical computers even without containing much entanglement.

In 2000-2001, Żurek et al. developed the concept of quantum discord – “a measure of the quantumness of correlations” [13,14]. Simultaneously and independently, Vedral et al. [15,16] proposed a measure for the purely classical correlation, which, after subtracting it from the total correlation, led to the same amount of quantum correlation as the discord. Then Datta et al. [17, 18] calculated discord in the Knill-Laflamme DQC1 model and showed that it scales with the quantum efficiency, while entanglement remains vanishingly small throughout the computation. This attracted a lot of attention to the new measure of quantum correlation [19,20,21,22,23].

Quantum discord and entanglement are the same for the pure quantum states. However discord can exist in separable mixed states, i.e., when quantum entanglement is identically equal to zero. The set of separable states possesses a nonzero volume in the whole Hilbert space of a system [24] (it is a necessary condition for the arising of entanglement sudden death (ESD) effect [25]), whereas the set of states with zero discord, *vice versa*, is negligibly small [26]. This circumstance alone sharply distinguishes discord from entanglement. Moreover, numerous theoretical and experimental investigations of different quantum system have clearly shown that while the quantum entanglement and discord measure the same thing – the quantum correlation, but as a matter of fact, discrepancies in quantitative and even qualitative behavior are very large [27,28,29]. Discord and entanglement behave differently even for simplest mixed states — the Werner and Bell-diagonal ones (see, e.g, [30]). This has led

¹ However, “it is important to realize that in physics today, we have no knowledge of what the energy *is*” [7].

² Earlier, a similar definition was proposed by Everett for the *canonical correlation* [11].

many to talk about entanglement and discord as different types of quantum correlations.

However, the subsequent proposals with more and more new measures of quantum correlations [31,32] caused a dilemma: should each measure be attributed to its own correlation, or should it be argued that there is only one quantum correlation, but the methods of describing it are not adequate? The physicists community now prefers to talk about entanglement and discord-like quantum correlations [33]. As is customary for brevity, we will also refer to the various measures of quantum correlation as “quantum correlations”. Nevertheless, the quantum correlation is one, but now there are only different measures of it, which are still imperfect. We would like to have such measures of quantum correlations that would be useful for estimating the values of the speedup of quantum computing, the efficiency of quantum heat engines, etc. Let the measures be different, but the results must be the same. (As, for example, there are various formulations of quantum mechanics which differ dramatically in mathematical and conceptual overview, yet each one makes identical predictions for all experimental results [34].)

In the present paper we study the behavior simultaneously of three measures of quantum correlation: entropic quantum discord, local quantum uncertainty, and local quantum Fisher information (definitions for them are given in the next section). Calculations are carried out using a fully anisotropic Heisenberg model of two spin-1/2 with taken into account the Dzyaloshinsky–Moriya (DM) and Kaplan–Shekhtman–Entin-Wohlman–Aharony (KSEA) interactions. The model is considered in thermal equilibrium with a thermal bath. Through extensive graphical analysis, we find that the behavior of these significantly different measures demonstrate a similar qualitative and, in many cases, acceptable quantitative agreement with each other.

The organization of this paper is as follows. We begin in Sect. 2 with a brief overview of the quantum correlation measures used in our work. The model is described in Sect. 3. Expressions for the quantum correlations are derived and presented in Sect. 4. Section 5 is devoted to a detail description and discussion of different effects in behavior of quantum correlations under question. Our main conclusions are summarized in Sect. 6.

2 Preliminaries

Here we recall some notions and equations that will be needed in the following sections.

2.1 Quantum discord

The entropic quantum discord Q for a bipartite quantum state ρ is defined as the minimum difference between two classically-equivalent expressions of the mutual information [14]: $Q(\rho) = I - J$, where I is the usual quantum

mutual information and J the local measurement-induced quantum mutual information. Below we will deal with the Bell-diagonal states. Exact explicit formula for the quantum discord of these quantum states has been derived by Luo [35]. Notice that another quantity of quantum correlation, namely the one-way quantum work deficit coincides the quantum discord in Bell-diagonal states (see, e.g., [36]).

2.2 Local quantum uncertainty

The local quantum uncertainty (LQU) as a measure of quantum correlation, \mathcal{U} , was appeared in 2013 [37] (see also [38] and references therein). It is defined as the minimum quantum uncertainty associated to a single measurement on one subsystem, say A , of bipartite system AB . The authors [37] have evaluated this measure in the case of $2 \times d$ systems:

$$\mathcal{U}(\rho) = 1 - \lambda_{max}(W), \quad (1)$$

where λ_{max} denotes the maximum eigenvalue of the 3×3 symmetric matrix W whose entries are

$$W_{\mu\nu} = \text{Tr}\{\rho^{1/2}(\sigma_\mu \otimes \mathbf{I})\rho^{1/2}(\sigma_\nu \otimes \mathbf{I})\} \quad (2)$$

with $\mu, \nu = x, y, z$ and $\sigma_{x,y,z}$ are the Pauli matrices.

2.3 Local quantum Fisher information

Fisher's concept of information [39] has a long history and wide applications [40, 41, 42, 43, 44]. A measure of nonclassical correlations based on it was suggested in 2014 [45] (see there especially Supplementary Information) under name "interferometric power"; see also [46]. This measure which we will denote by \mathcal{F} equals the optimal local quantum Fisher information (LQFI) F with the measuring operator H_A acting in the subspace of party A :

$$\mathcal{F}(\rho) = \min_{H_A} F(\rho, H_A). \quad (3)$$

3 Hamiltonian and density matrix

Consider a two-qubit fully anisotropic Heisenberg model with DM and KSEA interactions [47]. In a zero external field, Hamiltonian reads

$$\mathcal{H} = J_x \sigma_1^x \sigma_2^x + J_y \sigma_1^y \sigma_2^y + J_z \sigma_1^z \sigma_2^z + D_z (\sigma_1^x \sigma_2^y - \sigma_1^y \sigma_2^x) + \Gamma_z (\sigma_1^x \sigma_2^y + \sigma_1^y \sigma_2^x). \quad (4)$$

Its matrix form has the X structure:

$$\mathcal{H} = \begin{pmatrix} J_z & \cdot & \cdot & J_x - J_y - 2i\Gamma_z \\ \cdot & -J_z & J_x + J_y + 2iD_z & \cdot \\ \cdot & J_x + J_y - 2iD_z & -J_z & \cdot \\ J_x - J_y + 2i\Gamma_z & \cdot & \cdot & J_z \end{pmatrix}, \quad (5)$$

where the dots are put instead of zero entries. The energy levels are given as

$$E_{1,2} = J_z \pm r_1, \quad E_{3,4} = -J_z \pm r_2, \quad (6)$$

where

$$r_1 = [(J_x - J_y)^2 + 4\Gamma_z^2]^{1/2}, \quad r_2 = [(J_x + J_y)^2 + 4D_z^2]^{1/2}. \quad (7)$$

Note that Γ_z (constant of KSEA interaction) is accumulated only in r_1 , while the constant of DM coupling, D_z , is contained entirely in the coefficient r_2 .

The partition function $Z = \sum_i \exp(-\beta E_i)$ equals

$$Z = 2(e^{-\beta J_z} \cosh \beta r_1 + e^{\beta J_z} \cosh \beta r_2), \quad (8)$$

where $\beta = 1/T$ and T is the absolute temperature in energy units. The Gibbs density matrix is given as

$$\rho = \frac{1}{Z} \exp(-\beta \mathcal{H}). \quad (9)$$

Calculations yield

$$\rho = \begin{pmatrix} a & \cdot & \cdot & u \\ \cdot & b & v & \cdot \\ \cdot & v^* & b & \cdot \\ u^* & \cdot & \cdot & a \end{pmatrix} \quad (10)$$

(the asterisk denotes complex conjugation). Here

$$\begin{aligned} a &= \frac{1}{Z} e^{-\beta J_z} \cosh \beta r_1, & u &= -\frac{1}{Z} \frac{J_x - J_y - 2i\Gamma_z}{r_1} e^{-\beta J_z} \sinh \beta r_1, \\ b &= \frac{1}{Z} e^{\beta J_z} \cosh \beta r_2, & v &= -\frac{1}{Z} \frac{J_x + J_y + 2iD_z}{r_2} e^{\beta J_z} \sinh \beta r_2, \end{aligned} \quad (11)$$

where r_1 and r_2 are given again by Eq. (7).

Using the invariance of quantum correlations under any local unitary transformations (see, for example, [21]), we remove complex phases in the off-diagonal entries and change $\rho \rightarrow \varrho$, where

$$\varrho = \begin{pmatrix} a & \cdot & \cdot & |u| \\ \cdot & b & |v| & \cdot \\ \cdot & |v| & b & \cdot \\ |u| & \cdot & \cdot & a \end{pmatrix} \quad (12)$$

with

$$|u\rangle = \frac{1}{Z} e^{-\beta J_z} \sinh \beta r_1, \quad |v\rangle = \frac{1}{Z} e^{\beta J_z} \sinh \beta r_2. \quad (13)$$

Via orthogonal transformation

$$R = \frac{1}{\sqrt{2}} \begin{pmatrix} 1 & \cdot & \cdot & 1 \\ \cdot & 1 & 1 & \cdot \\ \cdot & 1 & -1 & \cdot \\ 1 & \cdot & \cdot & -1 \end{pmatrix} = R^t \quad (14)$$

(the subscript t stands for matrix transpose), the density matrix ϱ is reduced to the diagonal form

$$R\varrho R = \begin{pmatrix} p_1 & \cdot & \cdot & \cdot \\ \cdot & p_2 & \cdot & \cdot \\ \cdot & \cdot & p_3 & \cdot \\ \cdot & \cdot & \cdot & p_4 \end{pmatrix}, \quad (15)$$

where eigenvalues equal

$$p_1 = a + |u|, \quad p_2 = b + |v|, \quad p_3 = b - |v|, \quad p_4 = a - |u|. \quad (16)$$

The corresponding eigenvectors of ϱ are given as

$$|1\rangle = \frac{1}{\sqrt{2}} \begin{pmatrix} 1 \\ \cdot \\ \cdot \\ 1 \end{pmatrix}, \quad |2\rangle = \frac{1}{\sqrt{2}} \begin{pmatrix} \cdot \\ 1 \\ 1 \\ \cdot \end{pmatrix}, \quad |3\rangle = \frac{1}{\sqrt{2}} \begin{pmatrix} \cdot \\ 1 \\ -1 \\ \cdot \end{pmatrix}, \quad |4\rangle = \frac{1}{\sqrt{2}} \begin{pmatrix} 1 \\ \cdot \\ \cdot \\ -1 \end{pmatrix}. \quad (17)$$

These are the Bell vectors $|\Phi^+\rangle$, $|\Psi^+\rangle$, $|\Psi^-\rangle$, and $|\Phi^-\rangle$, respectively.

4 Expressions for the quantum correlations

The state (12) belongs to the Bell-diagonal family which in turn is a subclass of X quantum states. It is noteworthy that both entropic quantum discord and one-way quantum work deficit give the same results not only for the Bell diagonal states, but even for the X quantum states if the marginal state of one qubit is maximally mixed and measurements are performed on this qubit [36].

4.1 Quantum discord

Quantum discord in the case of Bell diagonal states can be written as [48, 49]

$$Q = \min\{Q_0, Q_1\}. \quad (18)$$

The branch Q_0 corresponds to the zero optimal measurement angle and is given as

$$Q_0 = -S - 2(a \log_2 a + b \log_2 b), \quad (19)$$

where a and b are determined by Eq. (11) and S is the entropy of the system in bits:

$$S \equiv - \sum_{i=1}^4 p_i \log_2 p_i = \log_2 Z - \frac{2\beta}{Z \ln 2} [e^{-\beta J_z} (r_1 \sinh \beta r_1 - J_z \cosh \beta r_1) + e^{\beta J_z} (r_2 \sinh \beta r_2 + J_z \cosh \beta r_2)]. \quad (20)$$

The second branch Q_1 corresponds to the $\pi/2$ optimal measurement angle and is expressed as

$$Q_1 = 1 - S - \frac{1+w}{2} \log_2 \frac{1+w}{2} - \frac{1-w}{2} \log_2 \frac{1-w}{2}, \quad (21)$$

where

$$w = 2(|u| + |v|) = \frac{2}{Z} (e^{-\beta J_z} \sinh \beta r_1 + e^{\beta J_z} \sinh \beta r_2). \quad (22)$$

The transition threshold from one branch to another is determined by the equation $Q_0 = Q_1$ or in open form,

$$\ln 2 + 2(a \ln a + b \ln b) - \frac{1+w}{2} \ln \frac{1+w}{2} - \frac{1-w}{2} \ln \frac{1-w}{2} = 0. \quad (23)$$

4.2 Optimal LQU

Using transformation (14) we get matrix elements $\langle m | \sigma_\mu \otimes I | n \rangle$ in the diagonal representation of the density matrix ρ :

$$R(\sigma_x \otimes I)R = \begin{pmatrix} . & 1 & . & . \\ 1 & . & . & . \\ . & . & . & -1 \\ . & . & -1 & . \end{pmatrix}, \quad (24)$$

$$R(\sigma_y \otimes I)R = \begin{pmatrix} . & . & i & . \\ . & . & . & i \\ -i & . & . & . \\ . & -i & . & . \end{pmatrix}, \quad (25)$$

$$R(\sigma_z \otimes I)R = \begin{pmatrix} . & . & . & 1 \\ . & . & 1 & . \\ . & 1 & . & . \\ 1 & . & . & . \end{pmatrix}. \quad (26)$$

From here, it is easy to see that the matrix W defined by Eq. (2) is diagonal and its eigenvalues are equal to (for a comparison, see, e.g., [50,51])

$$W_{xx} = 2(\sqrt{p_1 p_2} + \sqrt{p_3 p_4}) = 2(\sqrt{(a+|u|)(b+|v|)} + \sqrt{(a-|u|)(b-|v|)}), \quad (27)$$

$$W_{yy} = 2(\sqrt{p_1 p_3} + \sqrt{p_2 p_4}) = 2(\sqrt{(a+|u|)(b-|v|)} + \sqrt{(a-|u|)(b+|v|)}), \quad (28)$$

$$W_{zz} = 2(\sqrt{p_1 p_4} + \sqrt{p_2 p_3}) = 2(\sqrt{a^2 - |u|^2} + \sqrt{b^2 - |v|^2}). \quad (29)$$

In explicit form

$$W_{xx} = \frac{4}{Z} \cosh[\beta(r_1+r_2)/2], \quad W_{yy} = \frac{4}{Z} \cosh[\beta(r_1-r_2)/2], \quad W_{zz} = \frac{4}{Z} \cosh \beta J_z. \quad (30)$$

It is clear that $W_{xx} \geq W_{yy}$. Therefore, the value of quantum correlation trough LQU equals

$$\mathcal{U} = \min\{\mathcal{U}_0, \mathcal{U}_1\}, \quad (31)$$

where

$$\mathcal{U}_0 = 1 - W_{zz}, \quad \mathcal{U}_1 = 1 - W_{xx}. \quad (32)$$

4.3 Optimal LQFI

Local quantum Fisher information reads [45, 52, 53], [54]³, [55, 56]

$$F(\varrho, H_A) = \frac{1}{2} \sum_{m,n} \frac{(p_m - p_n)^2}{p_m + p_n} |\langle m|H_A|n \rangle|^2, \quad (33)$$

where the operator H_A acts in the subspace of party A . For qubit systems, one takes

$$H_A = \boldsymbol{\sigma} \cdot \mathbf{r} \quad (34)$$

with $|\mathbf{r}| = 1$; $\boldsymbol{\sigma} = (\sigma_x, \sigma_y, \sigma_z)$ is the vector of the Pauli matrices. The relation (details can be found in [52, 56])

$$\sum_{m \neq n} \frac{2p_m p_n}{p_m + p_n} |\langle m|H_A|n \rangle|^2 = \sum_{\mu, \nu=x,y,z} \sum_{m \neq n} \frac{2p_m p_n}{p_m + p_n} \langle m|\sigma_\mu \otimes I|n \rangle \langle n|\sigma_\nu \otimes I|m \rangle \quad (35)$$

leads to $\mathcal{F} = 1 - \lambda_{max}$, where λ_{max} is the largest eigenvalue of the real symmetric 3×3 matrix M with entries

$$M_{\mu\nu} = \sum_{m \neq n} \frac{2p_m p_n}{p_m + p_n} \langle m|\sigma_\mu \otimes I|n \rangle \langle n|\sigma_\nu \otimes I|m \rangle. \quad (36)$$

Using Eqs. (24)–(26), one finds that the matrix M is also diagonal and its nondiagonal elements (eigenvalues) are equal to

$$M_{xx} = \frac{4p_1 p_2}{p_1 + p_2} + \frac{4p_3 p_4}{p_3 + p_4} = \frac{4(a+|u|)(b+|v|)}{a+b+|u|+|v|} + \frac{4(a-|u|)(b-|v|)}{a+b-|u|-|v|}, \quad (37)$$

³ Note that the expressions for the density matrix elements and partition function, Eqs. (23) and (24) in Ref. [54], contain errors.

$$M_{yy} = \frac{4p_1p_3}{p_1 + p_3} + \frac{4p_2p_4}{p_2 + p_4} = \frac{4(a + |u|)(b - |v|)}{a + b + |u| - |v|} + \frac{4(a - |u|)(b + |v|)}{a + b - |u| + |v|}, \quad (38)$$

$$M_{zz} = \frac{4p_1p_4}{p_1 + p_4} + \frac{4p_2p_3}{p_2 + p_3} = \frac{2(a^2 - |u|^2)}{a} + \frac{2(b^2 - |v|^2)}{b}. \quad (39)$$

In explicit form,

$$\begin{aligned} M_{xx} &= \frac{4 e^{\beta J_z} \cosh \beta r_1 + e^{-\beta J_z} \cosh \beta r_2}{Z \cosh 2\beta J_z + \cosh[\beta(r_1 - r_2)]}, \\ M_{yy} &= \frac{4 e^{\beta J_z} \cosh \beta r_1 + e^{-\beta J_z} \cosh \beta r_2}{Z \cosh 2\beta J_z + \cosh[\beta(r_1 + r_2)]}, \\ M_{zz} &= \frac{2 e^{\beta J_z} \cosh \beta r_1 + e^{-\beta J_z} \cosh \beta r_2}{Z \cosh \beta r_1 \cosh \beta r_2}. \end{aligned} \quad (40)$$

It is seen that $M_{xx} \geq M_{yy}$. Hence, the value of the quantum correlation in terms of LQFI is defined by equation

$$\mathcal{F} = \min\{\mathcal{F}_0, \mathcal{F}_1\}, \quad (41)$$

where

$$\mathcal{F}_0 = 1 - M_{zz}, \quad \mathcal{F}_1 = 1 - M_{xx}. \quad (42)$$

4.4 Boundaries between branches

Equation for the boundary separating the regions with branches \mathcal{U}_0 and \mathcal{U}_1 is $\mathcal{U}_0 = \mathcal{U}_1$. Using Eqs. (30) and (32) we get the solution

$$r_1 + r_2 = 2|J_z|. \quad (43)$$

In turn, equation for the boundary between two branches \mathcal{F}_0 and \mathcal{F}_1 is also reduced to the condition (43). Moreover, performing direct calculations (by hand or using the package Mathematica) it is easy to prove that the transcendental equation (23) has a solution $|J_z| = (r_1 + r_2)/2$. It is remarkable that the branches of the three measures under study are separated by the same boundary (43).

The formulas presented in this section open a way to investigate the behavior of nonclassical correlations in the thermolyzed system (4).

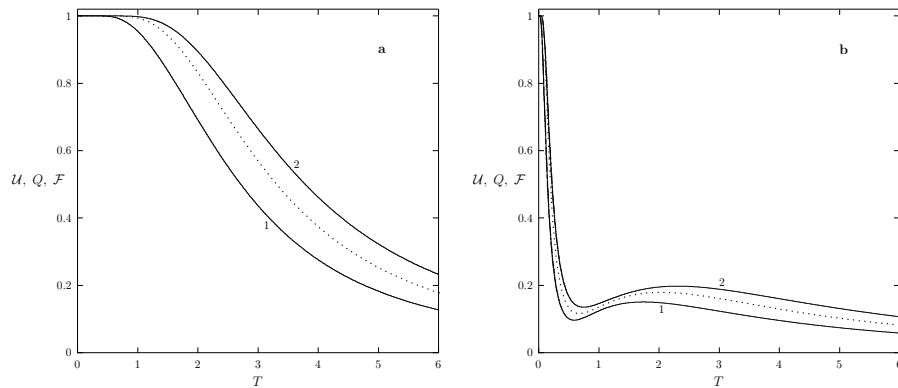


Fig. 1 Quantum correlations \mathcal{U} (solid line 1), Q (dotted line), and \mathcal{F} (solid line 2) versus temperature T for $J_x = -1$, $J_y = -1.5$, $D = 1.8$, $\Gamma_z = 0.3$ and $J_z = 2$ (a) and $J_z = -2$ (b)

5 Results and discussion

Before starting a general analysis, consider two examples with different behavior of quantum correlations. Figure 1, (a) and (b), shows the dependencies of LQU, discord Q , and LQFI as functions of temperature. Interaction constants J_x , J_y , D_z , and Γ_z are the same in both cases (a) and (b), while J_z differs only in sign: $J_z = 2$ (antiferromagnetic exchange coupling) and $J_z = -2$ (ferromagnetic exchange coupling).

One can see the following. All curves go to zero as the temperature rises. On the other hand, in the limit $T \rightarrow 0$, quantum correlations reach the maximum possible value equaling one and their first derivatives with respect to the temperature equals zero at $T = 0$. This leads to quasi-horizontal sections on the curves. Characteristic length (temperature) of these sections, T_{ch} , one could try to relate with the energy gap ΔE in the spectrum: $T_{ch} \sim \Delta E$. Using Eqs. (6) and (7) and numerical values of interaction constants given in the figure caption we obtain the estimations: $T_{ch,a} \sim 7.6$ for the dependencies in Fig. 1a and $T_{ch,b} \sim 0.4$ for the dependencies in Fig. 1b. Looking at the curves in the figure, we conclude that the estimates correctly give that the quasi-horizontal section in the antiferromagnetic case is much larger than in the ferromagnetic case. However, as can be seen from Fig. 1, both estimates give an order of magnitude overestimated values.

Next, the behavior of quantum correlations in Fig. 1a characterized by *monotonic* decrease from one to zero. We will refer to this behavior as type I behavior. It is noteworthy that the curves shown in Fig. 1b, also decrease from one to zero, but have local rise in the intermediate temperature range (approximately from $T_1 \approx 0.6$ to $T_2 \approx 2.2$). Such behavior with local minimum and maximum at $T > 0$ will be referred to as type II.

It is seen from Fig. 1 that the dependencies for temperatures $T \in (0, \infty)$ satisfy the inequalities $\mathcal{U} < \mathcal{Q} < \mathcal{F}$. Finally, the curves for both $J_z = 2$ and $J_z = -2$ repeat the behavior of each other quite well.

5.1 High-temperature behavior

The observed behavior at high temperatures can be confirmed by rigorous calculations. Using formulas for the different quantum correlations derived in the previous section, we obtain for the quantum discord

$$Q_0(T)|_{T \rightarrow \infty} = \frac{r_1^2 + r_2^2}{4T^2 \ln 2} + \frac{J_z(r_2^2 - r_1^2)}{4T^3 \ln 2} + O(1/T^4), \quad (44)$$

$$Q_1(T)|_{T \rightarrow \infty} = \frac{4J_z^2 + (r_1 - r_2)^2}{8T^2 \ln 2} + \frac{J_z(r_2^2 - r_1^2)}{4T^3 \ln 2} + O(1/T^4), \quad (45)$$

for the LQU

$$\mathcal{U}_0(T)|_{T \rightarrow \infty} = \frac{r_1^2 + r_2^2}{4T^2} + \frac{J_z(r_2^2 - r_1^2)}{4T^3} + O(1/T^4), \quad (46)$$

$$\mathcal{U}_1(T)|_{T \rightarrow \infty} = \frac{4J_z^2 + (r_1 - r_2)^2}{8T^2} + \frac{J_z(r_2^2 - r_1^2)}{4T^3} + O(1/T^4), \quad (47)$$

and for the LQFI

$$\mathcal{F}_0(T)|_{T \rightarrow \infty} = \frac{r_1^2 + r_2^2}{2T^2} + \frac{J_z(r_2^2 - r_1^2)}{2T^3} + O(1/T^4). \quad (48)$$

$$\mathcal{F}_1(T)|_{T \rightarrow \infty} = \frac{4J_z^2 + (r_1 - r_2)^2}{4T^2} + \frac{J_z(r_2^2 - r_1^2)}{2T^3} + O(1/T^4), \quad (49)$$

Thus, quantum correlations decay at high temperatures according to the law $1/T^2$.

5.2 Local unitary transformation of ϱ

As mentioned above, quantum correlations are invariant under any local unitary transformations. Let us take a local unitary (orthogonal) transformation $O = I \otimes \sigma_x$,

$$O = \begin{pmatrix} 1 & \cdot \\ \cdot & 1 \end{pmatrix} \otimes \begin{pmatrix} \cdot & 1 \\ 1 & \cdot \end{pmatrix} = \begin{pmatrix} \cdot & 1 & \cdot & \cdot \\ 1 & \cdot & \cdot & \cdot \\ \cdot & \cdot & \cdot & 1 \\ \cdot & \cdot & 1 & \cdot \end{pmatrix} = O^t. \quad (50)$$

Using it, the density matrix (12) is transformed as follows:

$$O\varrho O = \begin{pmatrix} b & \cdot & \cdot & |v| \\ \cdot & a & |u| & \cdot \\ \cdot & |u| & a & \cdot \\ |v| & \cdot & \cdot & b \end{pmatrix}. \quad (51)$$

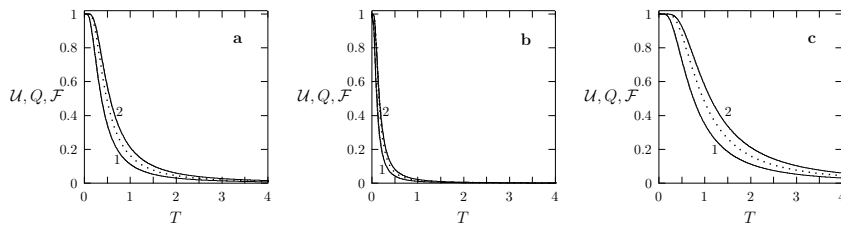


Fig. 2 Quantum correlations \mathcal{U} (solid line 1), Q (dotted line), and \mathcal{F} (solid line 2) as functions of temperature T for $J_z = 0$, $r_1 = 1$, and $r_2 = 0$ (a), 0.7 (b), and 3 (c)

This means that quantum correlations do not change upon exchange

$$\{J_z, r_1, r_2\} \leftrightarrow \{-J_z, r_2, r_1\}. \quad (52)$$

Thus, to describe all situations, it suffices to consider only the cases $J_z = 0$ and $J_z > 0$ for different values r_1 and r_2 (results for $J_z < 0$ will follow from results for $J_z > 0$ with simultaneous replace $r_1 \rightleftharpoons r_2$). We will consider both of these cases separately.

5.3 Case $J_z = 0$

Let us start with the zero value of the J_z interaction constant. Here the ground state energy is $E_0 = -\min\{r_1, r_2\}$ and the energy gap equals $|r_1 - r_2|$. Formulas for quantum correlations are greatly simplified. For instance,

$$\mathcal{U} = 1 - \operatorname{sech}[(r_1 - r_2)/2T] \quad (53)$$

and

$$\mathcal{F} = \tanh^2[(r_1 - r_2)/2T]. \quad (54)$$

The values of quantum correlations depend only on the relative distance $|r_1 - r_2|$ in the range for r_1 and r_2 from zero to infinity.

In fact, this case contains only one independent parameter. Without loss of generality, we put $r_1 = 1$ ($r_1 = 1$ will play the role of a normalization constant). The dependencies of quantum correlations are drawn in Fig. 2. It can be seen from this figure that the curves have a monotonically decreasing shape (refer to type I in our classification). When the single parameter r_2 increases from zero to one [see Fig. 2 (a) and (b)], the values of the quantum correlations decrease at given temperatures and completely vanish at $r_2 = 1$.

Indeed, for $r_2 = 1$ the energy spectrum, Eq. (6), consists of two levels $E_{1,2} = \pm 1$, which are both two-fold degenerate. At this point, the density matrix (12) takes the form

$$\varrho_0 = \begin{pmatrix} a & \cdot & \cdot & |u| \\ \cdot & a & |u| & \cdot \\ \cdot & |u| & a & \cdot \\ |u| & \cdot & \cdot & a \end{pmatrix}. \quad (55)$$

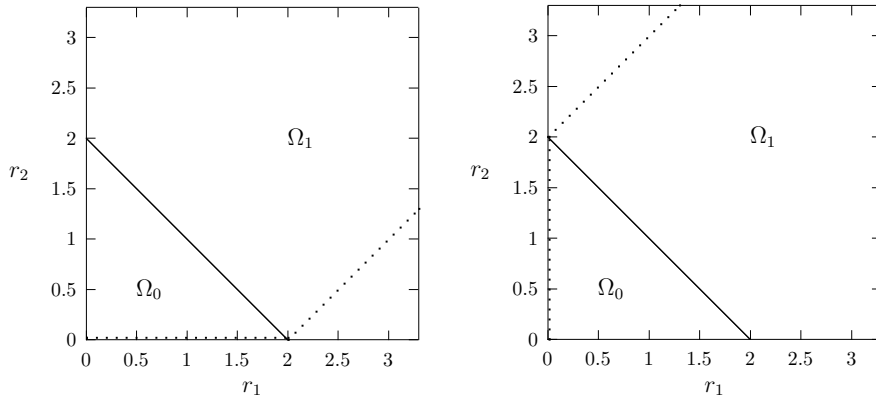


Fig. 3 Phase diagrams in the parameter space (r_1, r_2) for $J_z = 1$ (left) and $J_z = -1$ (right). Solid line $r_1 + r_2 = 2$ separates the regions Ω_0 and Ω_1 . Dotted broken lines [except points $(2, 0)$ and $(0, 2)$ in the left and right panels, respectively] show for which r_1 and r_2 quantum correlations vanish at $T = 0$

After the local unitary (orthogonal) transformation $H_2 = H \otimes H$, where

$$H = \frac{1}{\sqrt{2}} \begin{pmatrix} 1 & 1 \\ 1 & -1 \end{pmatrix} \quad (56)$$

is the Hadamard transform, the density matrix (55) is reduced to diagonal form: $H_2 \varrho_0 H_2 = \text{diag}(a + |u|, a - |u|, a - |u|, a + |u|)$. This means that the state (55) is classical and therefore all quantum correlations disappear. The latter is also seen from Eqs. (53) and (54).

With a further increase in r_2 , quantum correlations revive again, as seen in Fig. 2c.

5.4 Case $J_z \neq 0$

Taking J_z as a normalized constant and setting it equal to unity, the problem for the dependencies of quantum correlations on the dimensionless temperature T will contain two independent parameters r_1 and r_2 . The functions Q , \mathcal{U} , and \mathcal{F} are piecewise because each of them consist of two branches.

Figure 3 shows the domain for r_1 and r_2 , i.e., phase diagram in the plane (r_1, r_2) . The domain consists of two regions, Ω_0 (which corresponds to the branches Q_0 , \mathcal{U}_0 , and \mathcal{F}_0) and Ω_1 (which corresponds to the branches Q_1 , \mathcal{U}_1 , and \mathcal{F}_1), separated by the boundary (43) (solid line $r_1 + r_2 = 2$ in Fig. 3).

Consider the behavior of quantum correlations along the path $r_2 = 0$, i.e., on abscissa axis. At the origin of the Cartesian coordinates ($r_1 = r_2 = 0$), the off-diagonal elements of the density matrix ϱ , Eq. (12), equal zero, the system is classical and, therefore, quantum correlations are completely absent.

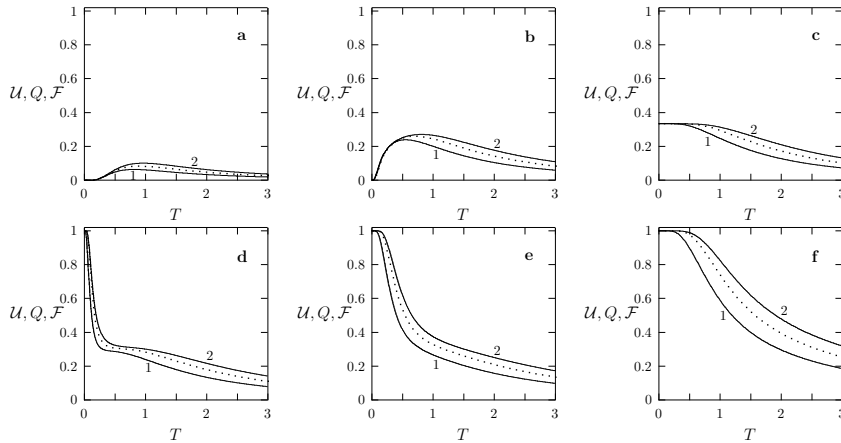


Fig. 4 U (solid line 1), Q (dotted line), and \mathcal{F} (solid line 2) vs T for $J_z = 1$, $r_2 = 0$, and $r_1 = 1$ (a), 1.8 (b), 2 (c), 2.3 (d), 3 (e), 5 (f)

If r_1 starts to increase, quantum correlations appear as depicted in Fig. 4a, and they grow with increasing r_1 , see Fig. 4b. These curves have hill-like form which preserves up to $r_1 = 2_{-0}$. We will refer to this behavior as behavior of type III. It is characterized by zero quantum correlations at $T = 0$ and nonzero at $T > 0$.

To understand this somewhat unexpected behavior, consider off-diagonal elements of the density matrix ϱ , Eq. (12). One off-diagonal element is $|v| = 0$, and the other, for $T \rightarrow 0$, has the form

$$|u| \approx \frac{1}{2} \frac{1}{1 + 2 \exp[(2 - r_1)/T]}. \quad (57)$$

It is clear that this quantity equals zero for $r_1 < 2$ in the low-temperature limit. In other words, at zero temperature the density matrix becomes diagonal and therefore all quantum correlations disappear. Interestingly enough, the system loses quantumness at zero temperature, whereas the same system contains nonclassical correlations for nonzero temperatures.

Observed behavior can also be established directly from the formulas for the quantum correlations. Indeed, for example, LQU on the abscissa in the Ω_0 region is given, according to Eqs. (30) and (32), as

$$U_0(T) = \frac{2 \sinh^2(r_1/2T)}{\cosh(r_1/T) + \exp(2/T)}. \quad (58)$$

When the temperature goes to zero, LQU behaves as

$$U_0(T) \approx \frac{1}{1 + 2 \exp[(2 - r_1)/T]}. \quad (59)$$

Hence it follows that $\mathcal{U}_0(0) \equiv 0$ for $r_1 \in [0, 2)$. Thus, the quantum correlation on the segment shown in Fig. 3 with a dotted horizontal line on the abscissa, is completely suppressed at absolute zero temperature. This is valid for other two correlations Q and \mathcal{F} , what is clear seen in Fig. 4 (a) and (b).

The third type of behavior of quantum correlations is radically different from the cases shown in Fig. 1, where quantum correlations at $T = 0$, on the contrary, reach the maximum possible value equal to unity (complete correlation). Note that similar hill-like behavior of quantum discord was earlier observed, e.g., in the spin systems with dipole-dipole interactions [57].

When r_1 reaches the value 2, a new qualitative change occurs in behavior of quantum correlations, namely, they are equal to one third ($1/3$) at zero absolute temperature. This follows from Eq. (59) and is clear seen in Fig. 4c. The value of quantum correlations here is not equal to zero or one at $T = 0$, correlations take an intermediate value. This is the IV type of behavior of quantum correlations.

With a further increase in the value of r_1 while maintaining $r_2 = 0$, LQU goes to another branch and becomes equal to

$$\mathcal{U}_1(T) = \frac{\cosh(r_1/T) + e^{2/T} - 2e^{1/T} \cosh(r_1/2T)}{\cosh(r_1/T) + e^{2/T}}. \quad (60)$$

At $r_1 = 2$, this equation also gives $\mathcal{U}_1 = 1/3$ in the low-temperature limit. However, when $r_1 > 2$, the values of quantum correlations jump from $1/3$ to one at zero temperature and have monotonically decreasing shapes for $T > 0$, as shown in Fig. 4d-f.

Let us now turn to the evolution of quantum correlations for $r_2 > 0$. Take, for example $r_2 = 0.1$, and let effective interaction r_1 increases from zero. The transformations of the curve shapes are shown in Fig. 5. The first thing we observe is a qualitative change in behavior at $r_1 = 0$, see Fig. 5a. When $r_2 > 0$, the quantum correlations at $T = 0$ are now equal to one rather than zero. Otherwise, the curves repeat the behavior of the second and first types.

However there is an unexpected exception at $r_1 = 2.1$, where the maximum at $T = 0$ suddenly disappears completely. This is shown in Fig. 5e. To establish the reason for this behavior, consider again the structure of quantum state ϱ in the limit $T \rightarrow 0$ under relation $r_1 - r_2 = 2$. For this purpose, take expressions for the diagonal, a and b , and off-diagonal matrix elements $|u|$ and $|v|$, Eqs. (11) and (13). Performing the necessary calculations, we obtain that the quantum state at zero temperature is written as

$$\varrho_1 = \frac{1}{4} \begin{pmatrix} 1 & . & . & 1 \\ . & 1 & 1 & . \\ . & 1 & 1 & . \\ 1 & . & . & 1 \end{pmatrix}. \quad (61)$$

Like (55), the given state is classical and, hence, all quantum correlations vanish at $T = 0$ on the line $r_2 = r_1 - 2$ (it is shown by dotted inclined line in Fig. 3). This phenomenon could be called the sudden death of quantum correlation at zero temperature.

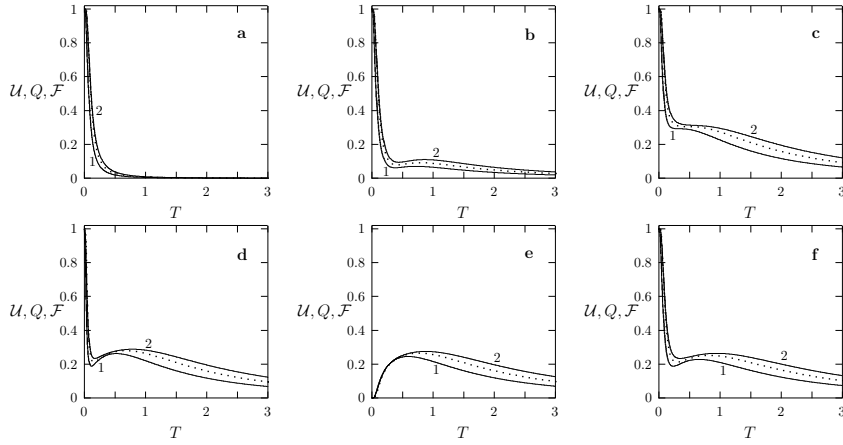


Fig. 5 \mathcal{U} (solid line 1), Q (dotted line), and \mathcal{F} (solid line 2) vs T for $J_z = 1$, $r_2 = 0.1$, and $r_1 = 0$ (a), 1 (b), 1.9 (c), 2 (d), 2.1 (e), 2.3 (f)

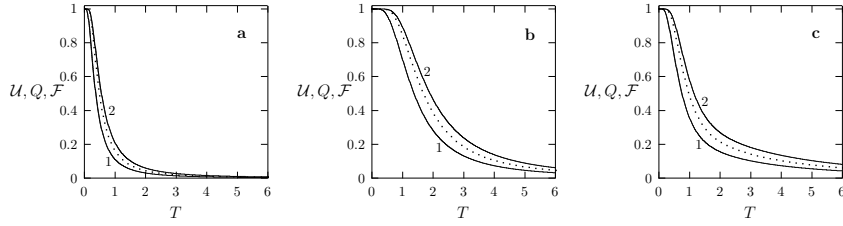


Fig. 6 Quantum correlations \mathcal{U} (solid line 1), Q (dotted line), and \mathcal{F} (solid line 2) versus temperature T for $J_z = 1$ and $r_1 = r_2 = 0.5$ (a); $r_1 = 0, r_2 = 2$ (b); $r_1 = 5, r_2 = 1$ (c)

In general, the following conclusion can be drawn. Dependencies of quantum correlations near neighborhoods of the dotted polyline (see Fig. 3) belong to the type II. Away from this line, the quantum correlation curves decrease monotonically without increase in any intermediate temperature range (type I of behavior). As an illustration, we depicted the dependencies of LQU, discord, and LQFI in Fig. 6 at a few randomly chosen point in the regions Ω_0 and Ω_1 and on the boundary between them (see again Fig. 3). Their behavior corresponds to type I.

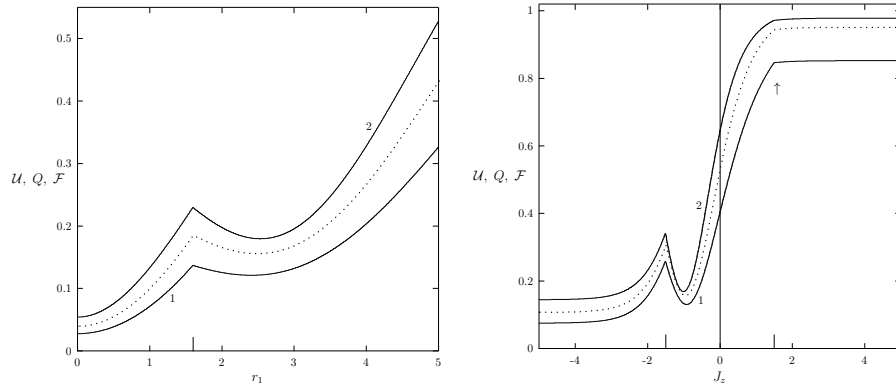


Fig. 7 \mathcal{U} (solid line 1), Q (dotted line), and \mathcal{F} (solid line 2) versus r_1 by $T = 1.5$, $J_z = 1$, $r_2 = 0.4$ (a) and versus J_z by $T = 1$, $r_1 = 0.4$, $r_2 = 2.6$ (b). Vertical arrow on the right panel indicates the position of fractures (sharp bends) on curves for $J_z = 1.5$

5.5 Sudden change phenomena of quantum correlations

5.5.1 $T > 0$

According to Eqs. (18), (31), and (41), the quantities Q , \mathcal{U} , and \mathcal{F} are determined by choice from two alternatives. This paves the way for the transitions of quantum correlations from one branch to another during the evolution of the system in some parameters. In catastrophe theory [58], such abrupt qualitative transitions with a smooth change in the control parameters are called sudden changes.

In the case under study, the situation is as follows. Since the boundary between the regions Ω_0 and Ω_1 does not depend on temperature, transitions from one branch to another do not occur at temperature changes. The interaction parameters need to be changed.

Figure 7a shows the behavior of quantum correlations versus the effective interaction parameter r_1 . It is clearly seen that all three dependencies have sharp maxima at $r_1 = 1.6$ (shown by a longer bar on the abscissa), where the first derivatives of quantum correlation functions with respect to r_1 undergo discontinuities of the first kind. The point of sudden changes, $r_1 = 1.6$, lies at the boundary $r_1 + r_2 = 2$ which separates the regions Ω_0 and Ω_1 (see Fig. 3).

Two sudden changes can be seen in Fig. 7b, where quantum correlation dependencies are presented as functions of the longitudinal interaction J_z . Transitions occur when $J_z = \pm 1.5$ (shown by two longer bars on the abscissa), which follow from the condition $r_1 + r_2 = 2|J_z|$. One group of sudden changes, at $J_z = -1.5$, looks as cusp-like peaks. Other sudden changes that occur when $J_z = 1.5$ are much less pronounced. They visible as weak fractures (kinks or bends), their position in the figure is marked arrow pointing up. All quantum

correlation functions are continuous, but their first derivatives with respect to the interaction J_z undergo finite jumps (discontinuities).

In practice, experimental measurements of fractures and jumps can be used to estimate the interaction parameters in the system.

5.5.2 $T = 0$

The above picture take place for nonzero temperatures. At $T = 0$, the measures of quantum correlation coincide, $\mathcal{U} = Q = \mathcal{F}$, and they can undergo discontinuities themselves. For example, when a completely cooled system evolves in r_2 along the trajectory $r_1 = 0$ (see Fig. 3), LQU changes as

$$\mathcal{U}(r_1 = 0, r_2) = \begin{cases} 0, & \text{if } r_2 = 0 \\ 1, & \text{if } r_2 > 0 \end{cases}. \quad (62)$$

This can be seen by comparing Fig. 4a and Fig. 5a. The same is valid for other two correlations, Q and \mathcal{F} .

On the path $r_2 = 0$, LQU versus r_1 changes as

$$\mathcal{U}(r_1, r_2 = 0) = \begin{cases} 0, & \text{if } r_1 < 2 \\ 1/3, & \text{if } r_1 = 2 \\ 1, & \text{if } r_1 > 2 \end{cases}. \quad (63)$$

Same for Q and \mathcal{F} as shown in Fig 4b-d at $T = 0$.

Such abrupt changes in quantum correlations can be attributed to quantum phase transitions.

6 Conclusions

In this paper, the two-qubit Heisenberg XYZ model with both antisymmetric Dzyaloshinsky–Moriya and symmetric Kaplan–Shekhtman–Entin-Wohlman–Aharony interactions has been considered at thermal equilibrium. For it, we have examined the behavior of three measures of quantum correlation, namely, the entropic quantum discord, local quantum uncertainty, and local quantum Fisher information. To classify the behavior of correlations, four qualitatively different types of curves have been suggested.

Despite the different underlying concepts behind quantum correlations, the comparative analysis showed good agreement between all measures. This is clearly evidenced by all the graphic material presented in Figs. 1, 2, and 4-7. That is, these measures are reduced to some one effective average measure. The entropic quantum discord Q could be taken as such an average measure, because it lies between two other measures: $\mathcal{U} \leq Q \leq \mathcal{F}$.

Park [59] has found that for the ferromagnetic case ($J_z < 1$; cf. Figs. 1 and 3, right), the thermal discord in the small T region exhibits a local minimum due to the DM interaction. In addition to this observation, we have established that local minima and maxima can also appear in the antiferromagnetic case, and they are caused by the KSEA interactions.

Next, all three measures as function of temperature are continuous and smooth. On the other hand, at nonzero temperatures, quantum correlations can suddenly change with a smooth change in the coupling parameters. Such abrupt changes are accompanied by fractures in the curves of quantum correlations. Moreover, we have found that the quantum correlations themselves can exhibit discontinuities at zero temperature.

Summing up, we conclude the following. In spin systems with DM and KSEA interactions, very similar behavior is observed for three different measures of nonclassical correlations: for the entropic quantum discord and measures based on the Fischer and Wigner-Yanase information.

References

1. Preskill, J.: Lecture Notes for Physics 229: Quantum Information and Computation. California Institute of Technology (1998), <http://www.theory.caltech.edu/~preskill/ph229>
2. Nielsen, M.A., Chuang, I.L.: Quantum Computation and Quantum Information. Cambridge University Press, Cambridge (2000)
3. Gisin, N., Ribordy, G., Tittel, W., Zbinden, H.: Quantum cryptography. *Rev. Mod. Phys.* **74**, 145 (2002)
4. Amico, L., Fazio, R., Osterloh, A., Vedral, V.: Entanglement in many-body systems. *Rev. Mod. Phys.* **80**, 517 (2008)
5. Horodecki, R., Horodecki, P., Horodecki, M., Horodecki, K.: Quantum entanglement. *Rev. Mod. Phys.* **81**, 865 (2009)
6. Reid, M.D., Drummond, P.D., Bowen, W.P., Cavalcanti, E.G., Lam, P.K., Bachor, H.A., Andersen, U.L., Leuchs, G.: Colloquium: The Einstein-Podolsky-Rosen paradox: From concepts to applications. *Rev. Mod. Phys.* **81**, 1727 (2009)
7. Feynman, R.P., Leighton, R.B., Sands, M.: The Feynman lectures on physics. Vol. 1, Sect. 4-1. Addison-Wesley, Reading, Mass. (1964)
8. Bennett, C.H., Brassard, G., Popescu, S., Schumacher, B., Smolin, J.A., Wootters, W.K.: Purification of noisy entanglement and faithful teleportation via noisy channels. *Phys. Rev. Lett.* **76**, 722 (1996); Erratum in: *Phys. Rev. Lett.* **78**, 2031 (1997)
9. Bennett, C.H., Bernstein, H.J., Popescu, S., Schumacher, B.: Concentrating partial entanglement by local operations. *Phys. Rev. A* **53**, 2046 (1996)
10. Bennett, C.H., DiVincenzo, D.P., Smolin, J.A., Wootters, W.K.: Mixed-state entanglement and quantum error correction. *Phys. Rev. A* **54**, 3824 (1996)
11. Everett III, E.: The theory of the universal wave function. In: *The Many-Worlds Interpretation of Quantum Mechanics*. Edited by B. S. DeWitt and N. Graham. Princeton University Press, Princeton, N.J. (1973)
12. Knill, E., Laflamme, R.: Power of one bit of quantum information. *Phys. Rev. Lett.* **81**, 5672 (1998)
13. Zurek, W.H.: Einselection and decoherence from an information theory perspective. *Ann. Phys. (Leipzig)* **9**, 855 (2000)
14. Ollivier, H., Zurek, W.H.: Quantum discord: a measure of the quantumness of correlations. *Phys. Rev. Lett.* **88**, 017901 (2001)
15. Henderson, L., Vedral, V.: Classical, quantum and total correlations. *J. Phys. A: Math. Gen.* **34**, 6890 (2001)
16. Vedral, V.: Classical correlations and entanglement in quantum measurements. *Phys. Rev. Lett.* **90**, 050401 (2003)
17. Datta, A.: Studies on the role of entanglement in mixed-state quantum computation. Dissertation. The University of New Mexico, Albuquerque (2008), arXiv:0807.4490v1 [quant-ph]
18. Datta, A., Shaji, A., Caves, C.M.: Quantum discord and the power of one qubit. *Phys. Rev. Lett.* **100**, 050502 (2008)
19. Merali, Z.: Quantum computing: The power of discord. *Nature* **474**, 24–26 (2011)

20. Modi, K., Brodutch, A., Cable, H., Paterek, T., Vedral, V.: Quantum discord and other measures of quantum correlation. arXiv:1112.6238v1 [quant-ph]
21. Modi, K., Brodutch, A., Cable, H., Paterek, T., Vedral, V.: The classical-quantum boundary for correlations: discord and related measures. *Rev. Mod. Phys.* **84**, 1655 (2012)
22. Aldoshin, S. M., Fel'dman, E. B., Yurischev, M. A.: Quantum entanglement and quantum discord in magnetoactive materials (Review Article). *Fiz. Nizk. Temp.* **40**, 5 (2014) [in Russian]; *Low Temp. Phys.* **40**, 3 (2014) [in English]
23. Streltsov, A.: *Quantum Correlations beyond Entanglement and Their Role in Quantum Information Theory*. SpringerBriefs in Physics. Springer, Berlin (2015)
24. Życzkowski, K., Horodecki, P., Sanpera, A., Lewenstein, M.: Volume of the set of separable states. *Phys. Rev. A* **58**, 883 (1998)
25. Yu, T., Eberly, J.H.: Sudden death of entanglement. *Science* **323**, 598 (2009)
26. Ferraro, A., Aolita, L., Cavalcanti, D., Cucchietti, F.M., Acín, A.: Almost all quantum states have nonclassical correlations. *Phys. Rev. A* **81**, 052318 (2010)
27. Werlang, T., Rigolin, G.: Thermal and magnetic quantum discord in Heisenberg models. *Phys. Rev. A* **81**, 044101 (2010)
28. Guo, J.-L., Mi, Y.-J., Zhang, J., Song, H.-S.: Thermal quantum discord of spins in an inhomogeneous magnetic field. *J. Phys. B: At. Mol. Opt. Phys.* **44**, 065504 (2011)
29. Campbell, S., Richens, J., Lo Gullo, N., Busch, T.: Criticality, factorization and long-range correlations in the anisotropic XY-model. *Phys. Rev. A* **88**, 062305 (2013)
30. Moreva, E., Gramegna, M., Yurischev, M.A.: Exploring quantum correlations from discord to entanglement. *Adv. Sci. Eng. Med.* **9**, 46 (2017)
31. Adesso, G., Bromley, T.R., Cianciaruso, M.: Measures and applications of quantum correlations (Topical review). *J. Phys. A: Math. Theor.* **49**, 473001 (2016)
32. Bera, A., Das, T., Sadhukhan, D., Roy, S.S., Sen(De), A., Sen, U.: Quantum discord and its allies: a review of recent progress. *Rep. Prog. Phys.* **81**, 024001 (2018)
33. Brodutch, A., Terno, D.R.: Why should we care about quantum discord? *In: Lectures on General Quantum Correlations and Their Applications*. Fanchini, F.F., Soares-Pinto, D.O., Adesso, G. (eds.) Springer, Berlin (2017)
34. Styer, D.F., Balkin, M.S., Becker, K.M., Burns, M.R., Dudley, C.E., Forth, S.T., Gaumer, J.S., Kramer, M.A., Oertel, D.C., Park, L.H., Rinkoski, M.T., Smith, C.T., Wotherspoon, T.D.: Nine formulations of quantum mechanics. *Am. J. Phys.* **70**, 288 (2002)
35. Luo, S.: Quantum discord for two-qubit systems. *Phys. Rev. A* **77**, 042303 (2008)
36. Ye, B.-L., Fei, S.-M.: A note on one-way quantum deficit and quantum discord. *Quantum Inf. Process.* **15**, 279 (2016)
37. Ghorami, D., Tufarelli, T., Adesso, G.: Characterizing nonclassical correlations via local quantum uncertainty. *Phys. Rev. Lett.* **110**, 240402 (2013)
38. Khedif, Y., Haddadi, S., Pourkarimi, M.R., Daoud, M.: Thermal correlations and entropic uncertainty in a two-spin system under DM and KSEA interactions. *Mod. Phys. Lett. A* **36**, 2150209 (2021)
39. Fisher, R.A.: Theory of statistical estimation. *Math. Proc. Cambridge Phil. Soc.* **22**, 700 (1925)
40. Efron, B.: R. A. Fisher in the 21st century. *Statist. Sci.* **13**, 95 (1998)
41. Petz, D., Ghinea, C.: Introduction to quantum Fisher information. In: *Quantum Probability and Related Topics*. World Scientific, Singapore (2011); arXiv:1008.2417v1 (2010)
42. Ly, A., Marsman, M., Verhagen, J., Grasman, R., Wagenmakers, E.-J.: A tutorial on Fisher information. arXiv:1705.01064v2 (2017)
43. Modi, K., Cable, H., Williamson, M., Vedral, V.: Quantum correlations in mixed-state metrology. *Phys. Rev. X* **1**, 021022 (2011)
44. R. Jafari, R., Akbari, A.: Dynamics of quantum coherence and quantum Fisher information after a sudden quench. *Phys. Rev. A* **101**, 062105 (2020)
45. Girolami, D., Souza, A.M., Giovannetti, V., Tufarelli, T., Filgueiras, J.G., Sarthour, R.S., Soares-Pinto, D.O., Oliveira, I.S., Adesso, G.: Quantum discord determines the interferometric power of quantum states. *Phys. Rev. Lett.* **112**, 210401 (2014); arXiv:1309.1472v4 (2014)
46. Kim, S., Li, L., Kumar, A., Wu, J.: Characterizing nonclassical correlations via local quantum Fisher information. *Phys. Rev. A* **97**, 032326 (2018)

47. Yurischev, M.A.: On the quantum correlations in two-qubit XYZ spin chains with Dzyaloshinsky–Moriya and Kaplan–Shekhtman–Entin-Wohlman–Aharony interactions. *Quantum Inf. Process.* **19**:336 (2020)
48. Yurischev, M.A.: On the quantum discord of general X states. *Quantum Inf. Process.* **14**:3399 (2015)
49. Fanchini, F.F., Werlang, T., Brasil, C.A., Arruda, L.G.E., Caldeira, A.O.: Non-Markovian dynamics of quantum discord. *Phys. Rev. A* **81**, 052107 (2010)
50. Jebli, L., Benzimoun, B., Daoud, M.: Quantum correlations for two-qubit X states through the local quantum uncertainty. *Int. J. Quant. Inf.* **15**, 1750020 (2017)
51. Guo, Y.-N., Peng, H.-P., Tian, Q.-L., Tan, Z.-G., Chen, Y.: Local quantum uncertainty in a two-qubit Heisenberg spin chain with intrinsic decoherence. *Phys. Scr.* **96**, 075101 (2021)
52. Bera, M.N.: Role of quantum correlation in metrology beyond standard quantum limit. arXiv:1405.5357v2 (2014)
53. Slaoui, A., Bakmou, L., Daoud, M., Ahl Laamara, R.: A comparative study of local quantum Fisher information and local quantum uncertainty in Heisenberg XY model. *Phys. Lett. A* **383**, 2241 (2019)
54. Haseli, S.: Local quantum Fisher information and local quantum uncertainty in two-qubit Heisenberg XYZ chain with Dzyaloshinskii-Moriya interactions. *Laser Phys.* **30**, 105203 (2020)
55. Muthuganesan, R., Chandrasekar, V. K.: Quantum Fisher information and skew information correlations in dipolar spin system. arXiv:2011.05879v1 (2020)
56. Ye, B.-L., Li, B., Liang, X.-B., Fei, S.-M.: Local quantum Fisher information and one-way quantum deficit in spin- $\frac{1}{2}$ XX Heisenberg chain with three-spin interaction. *Int. J. Quant. Inf.* **18**, 2050016 (2020)
57. Kuznetsova, E.I., Yurischev, M.A.: Quantum discord in spin systems with dipole-dipole interaction. *Quantum Inf. Process.* **12**:3587 (2013)
58. Arnold, V.I.: Catastrophe theory. Nauka, Moskva (1990) [in Russian], Springer, Berlin (1992) [in English]
59. Park, D.: Thermal entanglement and thermal discord in two-qubit Heisenberg XYZ chain with Dzyaloshinskii-Moriya interactions. *Quantum Inf. Process.* **18**:172 (2019)